Rigid-Flexible Body Analysis Without Rotation Parameters

R. L. Taylor

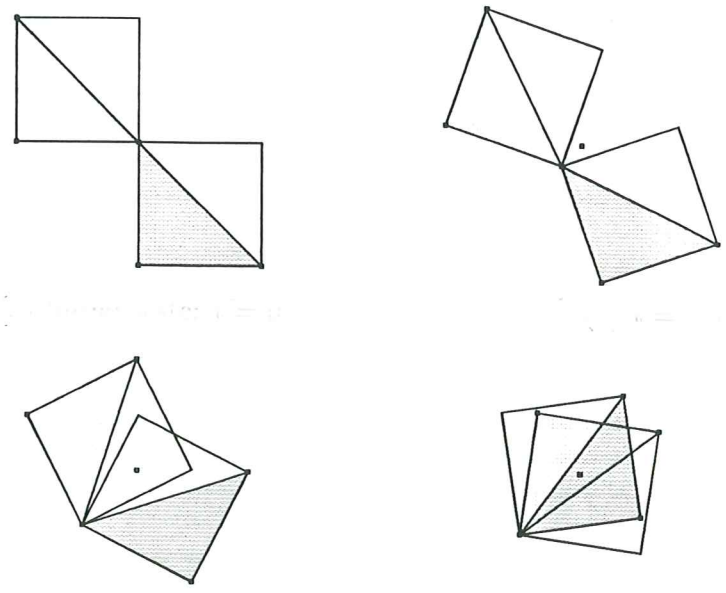

Publication CIMNE Nº 189, May 2000

Rigid-Flexible Body Analysis Without Rotation Parameters

R. L. Taylor

Publication CIMNE Nº 189, May 2000

International Center for Numerical Methods in Engineering

Gran Capitán s/n, 08034 Barcelona, Spain

Rigid-Flexible Body Analysis Without Rotation Parameters

R.L. Taylor *

Abstract

This paper addresses the coupled flexible and rigid body response of solids undergoing large motions and deformations. The formulation is presented in a form which is free of rotation parameters and thus avoids the need of finding compatible integration formulae for translations and rotations. The motion of each rigid body is represented in terms of the nodal parameters of a simplex element subject to constraints which ensure rigid motions. Flexible structural members for rods and shells are then expressed in terms of displacement and relative displacement parameters leading to total system of equations involving only translation degrees of freedom.

The motion are integrated using classical energy and momentum conserving schemes, thus leading to systems which are unconditionally stable for Hamiltonian (elastic-rigid) systems. The only requirement for absolute stability is that the non-linear algebraic equations representing the solution at each time step must converge.

The formulation is illustrated in two dimensions by representative numerical problems which involve both rigid and flexible parts or multi-rigid body situations. In all cases the conservation properties are observed.

1 Introduction

Many situations are encountered where treatment of the entire system as deformable bodies is neither necessary nor practical. For example, the frontal impact of a vehicle against a barrier requires a detailed modeling of the front part of the vehicle but the primary function of the engine and the rear part is to provide inertia – deformation being negligible for purposes of modeling the frontal impact. A second example, from geotechnical engineering, is the modeling of rock mass landslides or interaction between rocks on a conveyor belt where deformation of individual blocks is secondary.

The above problem classes divide themselves into two classes: One where it is necessary to include some simple mechanisms of deformation in each body (e.g., an individual rock piece) and the second in which the individual bodies have no deformation at all. The first class is called *pseudo-rigid* body deformation[1] and the second *rigid-body* behavior.[2] For the modeling of pseudo-rigid body analyses the reader is referred to the work of Cohen

*Professor in the Graduate School, Department of Civil and Environmental Engineering, University of California at Berkeley also Visiting Professor, CIMNE, Barcelona, Spain. e-mail: rlt@ce.berkeley.edu

and Muncaster.[1] A treatment of this formulation by a finite element method has been considered by Solberg and Papadopoulos[3] and an alternative form for motions restricted to incrementally linear behavior has been developed by Shi[4] and the method is commonly called *Discontinuous Deformation Analysis* (DDA). The DDA form, while widely used in the geotechnical community, is usually combined with a simple linear elastic constitutive model and linear strain-displacement forms which lead to large errors when finite rotations are encountered.

The literature on rigid body analysis is extensive with many books devoted to the subject (e.g., see references [2] and [5]) In addition there are many papers devoted exclusively to this subject and here, for example, we refer the reader to papers for additional details on numerical methods and formulations beyond those covered here.[6]-,[24] In this work we illustrate how rigid-body behavior can be described and combined in a finite element system. Two approaches are introduced, the first being one in which the motion of the rigid body is described by a translation and an orthogonal tensor representing rigid rotations. In the second approach we introduce a form which can be expressed entirely in terms of translations.

2 Equations for rigid bodies

Points in the deformed position of a body are denoted by $\mathbf{x}$ and are defined in terms of points in the a fixed inertial reference system $\mathbf{X}$ through the mapping (Fig. 1)

$$\mathbf{x} = \boldsymbol{\phi}(\mathbf{X}, t) \tag{1}$$

The material velocity is given as the time derivative of the motion

$$\mathbf{V} = \dot{\mathbf{x}} = \dot{\boldsymbol{\phi}}(\mathbf{X}, t) \tag{2}$$

where

$$\dot{\mathbf{x}} = \frac{\partial \boldsymbol{\phi}}{\partial t} \equiv \frac{\partial \mathbf{x}}{\partial t} \tag{3}$$

denotes partial differentiation with respect to time with $\mathbf{X}$ held fixed.

The position in the deformed configuration may be written in terms of a displacement $\mathbf{U}$ as[1]

$$\mathbf{x} = \mathbf{X} + \mathbf{U} \tag{4}$$

The change in shape of a solid body undergoing the motion $\boldsymbol{\phi}$ may be described in terms of the deformation gradient

$$\mathbf{F} = \frac{\partial \boldsymbol{\phi}}{\partial \mathbf{X}} = \mathbf{1} + \frac{\partial \mathbf{U}}{\partial \mathbf{X}} \tag{5}$$

in which $\mathbf{1}$ is a second order identity tensor. For a deformable body the Green-Lagrange strain tensor is then expressed as

$$\mathbf{E} = \frac{1}{2}\left(\mathbf{F}^T\mathbf{F} - \mathbf{1}\right) \tag{6}$$

and may be used in constitutive equations to define the second Piola-Kirchhoff stress, $\mathbf{S}$.

[1] A slight abuse of notation is used since normally a shifter is introduced to transform components between reference and current states. For simplicity, however, the shifter is omitted here.

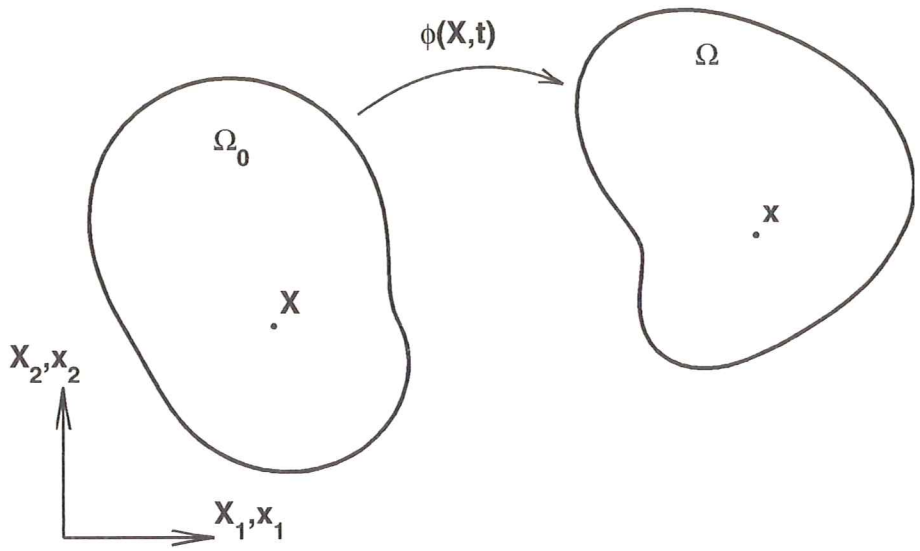

Figure 1: Reference and deformed (current) configuration for finite deformation problems

2.1 Weak form for rigid body motion

The weak form of the balance of momentum equation for a solid body undergoing large motions and deformations may be written in a reference configuration form as

$$\delta\Pi = \frac{\partial}{\partial t}\left(\int_\Omega \delta\mathbf{U}^T \rho_0 \, \mathbf{V} \, \mathrm{d}\Omega\right) + \int_\Omega \delta\mathbf{E}^T\mathbf{S} \, \mathrm{d}\Omega - \delta\Pi_{ext} = 0 \tag{7}$$

in which ρ_0 is the mass density at the reference state, $\delta(\cdot)$ denotes a variation (or virtual) quantity, and Π_{ext} is the effect of external loading. For conservative loading the external term may be written as

$$\delta\Pi_{ext} = \int_\Omega \delta\mathbf{U}^T \mathbf{b}_v \, \mathrm{d}\Omega + \int_{\Gamma_t} \delta\mathbf{U}^T \bar{\mathbf{T}} \, \mathrm{d}\Omega \tag{8}$$

in which $\mathbf{b}_v$ is a body force per unit of volume and $\bar{\mathbf{T}}$ a specified boundary traction on the part Γ_t. Points on Γ_u ($\Gamma_u \cup \Gamma_t \equiv \Gamma$) are assumed to have specified position or displacement given by

$$\mathbf{U} = \bar{\mathbf{U}} \quad \text{or} \quad \mathbf{x} = \bar{\mathbf{x}} \tag{9}$$

For a rigid body the balance of momentum equation becomes

$$\delta\Pi = \frac{\partial}{\partial t}\left(\int_\Omega \delta\mathbf{U}^T \rho_0 \, \mathbf{V} \, \mathrm{d}\Omega\right) - \delta\Pi_{ext} = 0 \tag{10}$$

subject to the constraint

$$\mathbf{E} = \mathbf{0} \tag{11}$$

2.2 Rigid bodies using translation and rotation parameters

Traditionally, the constraint given by Eq. (11) is satisfied by representing points in the current configuration by the mapping[25]

$$\mathbf{x} = \mathbf{r}(t) + \mathbf{\Lambda}(t)\,(\mathbf{X} - \mathbf{R}) \tag{12}$$

in which $\mathbf{R}$ is a position of a point in the reference body with respect to the fixed inertial frame and $\mathbf{r}$ is the position of the same point in the current configuration. In addition, $\mathbf{\Lambda}$ is an orthogonal second order tensor which describes the orientation of the rigid body relative to the fixed inertial frame (Fig. 2).

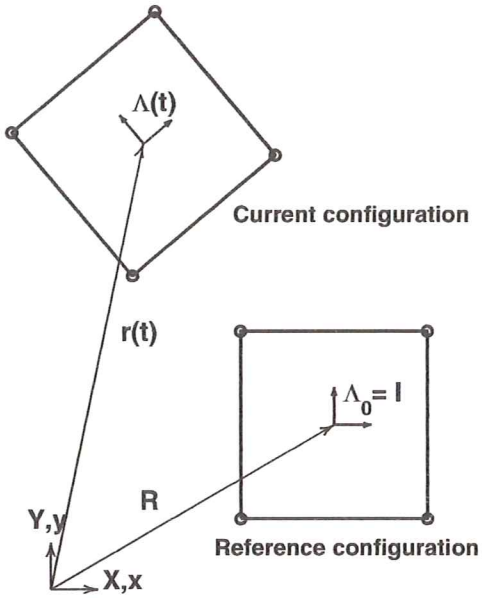

Figure 2: Motion for rigid body in terms of translation and rotation

Upon noting Eq. (4) we have

$$\delta\mathbf{x} = \delta\mathbf{U} \tag{13}$$

Using Eq. (12) we then obtain the velocity

$$\begin{aligned} \mathbf{V} &= \dot{\mathbf{r}} + \widehat{\boldsymbol{\omega}}\mathbf{\Lambda}\,(\mathbf{X} - \mathbf{R}) \\ &= \dot{\mathbf{r}} - (\widehat{\mathbf{x} - \mathbf{r}})\,\boldsymbol{\omega} \end{aligned} \tag{14}$$

and variation

$$\begin{aligned} \delta\mathbf{x} &= \delta\mathbf{r} + \delta\widehat{\boldsymbol{\theta}}\mathbf{\Lambda}\,(\mathbf{X} - \mathbf{R}) \\ &= \delta\mathbf{r} - (\widehat{\mathbf{x} - \mathbf{r}})\,\delta\boldsymbol{\theta} \end{aligned} \tag{15}$$

in which $\widehat{(\cdot)}$ denotes a skew symmetric matrix, $\boldsymbol{\omega}$ is the spatial angular velocity and $\delta\boldsymbol{\theta}$ is an arbitraty angular variation.

A skew symmetric matrix is an alternative way of representing the vector cross product which we notes induces the following properties

$$\widehat{\boldsymbol{\omega}}\,\mathbf{h} \equiv \boldsymbol{\omega} \times \mathbf{h} = -\,\mathbf{h} \times \boldsymbol{\omega} = -\widehat{\mathbf{h}}\,\boldsymbol{\omega} = \widehat{\mathbf{h}}^T\,\boldsymbol{\omega} \tag{16}$$

The last fact results from the fact that a skew symmetric matrix has the property

$$\widehat{\mathbf{h}} = -\widehat{\mathbf{h}}^T \tag{17}$$

as can be easily shown. We note that Eq. (16) introduces both the skew symmetric form of the rotation and the *rotation vector* which gives the representations

$$\boldsymbol{\omega} = \begin{bmatrix} \omega_1 & \omega_2 & \omega_3 \end{bmatrix}^T \quad \text{and} \quad \widehat{\boldsymbol{\omega}} = \begin{bmatrix} 0 & -\omega_3 & \omega_2 \\ \omega_3 & 0 & -\omega_1 \\ -\omega_2 & \omega_1 & 0 \end{bmatrix} \tag{18}$$

Assuming that $\mathbf{R}$ is placed at the center of mass, the momentum equation for a rigid body now becomes

$$\delta\Pi = \frac{\partial}{\partial t}\int_\Omega \left[\delta\mathbf{r}^T\,\rho_0\,\dot{\mathbf{r}} + \delta\boldsymbol{\theta}^T(\widehat{\mathbf{x}-\mathbf{r}})^T(\widehat{\mathbf{x}-\mathbf{r}})\boldsymbol{\omega}\right]\,\mathrm{d}\Omega - \delta\Pi_{ext} = 0 \tag{19}$$

in which now $\boldsymbol{\omega}$ is a vector of the angular velocity components. Defining the total mass of the body as

$$m = \int_\Omega \rho_0\,\mathrm{d}\Omega \tag{20}$$

and the spatial inertia tensor as

$$\mathcal{I} = \int_\Omega \rho_0\,(\widehat{\mathbf{x}-\mathbf{r}})^T(\widehat{\mathbf{x}-\mathbf{r}})\,\mathrm{d}\Omega \tag{21}$$

this simplifies to

$$\begin{aligned} \delta\Pi &= \frac{\partial}{\partial t}\left[\delta\mathbf{r}^T\,m\,\dot{\mathbf{r}} + \delta\boldsymbol{\theta}^T\mathcal{I}\boldsymbol{\omega}\right] - \delta\Pi_{ext} = 0 \\ &= \delta\mathbf{r}^T\,m\,\ddot{\mathbf{r}} + \delta\boldsymbol{\theta}^T\frac{\partial}{\partial t}\left(\mathcal{I}\boldsymbol{\omega}\right) - \delta\Pi_{ext} = 0 \end{aligned} \tag{22}$$

We note that the expression for computing the spatial inertia tensor may also be expressed as

$$\mathcal{I} = \int_\Omega \rho_0\,\left[(\mathbf{y}^T\mathbf{y})\,\mathbf{I} - \mathbf{y}\,\mathbf{y}^T\right]\,\mathrm{d}\Omega \tag{23}$$

where

$$\mathbf{y} = \mathbf{x} - \mathbf{r} \tag{24}$$

This may now be expressed in terms of the reference configutation inertia tensor $\mathcal{J}$ as

$$\begin{aligned} \mathcal{I} &= \mathbf{\Lambda}^T \left(\int_\Omega \left[(\mathbf{Y}^T\mathbf{Y})\,\mathbf{I} - \mathbf{Y}\,\mathbf{Y}^T \right] \mathrm{d}\Omega \right) \mathbf{\Lambda} \\ &= \mathbf{\Lambda}^T \mathcal{J}\, \mathbf{\Lambda} \end{aligned} \tag{25}$$

where similar to Eq. (24)

$$\mathbf{Y} = \mathbf{X} - \mathbf{R} \tag{26}$$

From the above we obtain for an individual rigid body the two equations

$$\frac{\mathrm{d}\mathbf{p}}{\mathrm{d}t} = \mathbf{f}_r \tag{27}$$

and

$$\frac{\mathrm{d}\boldsymbol{\pi}}{\mathrm{d}t} = \mathbf{m}_r \tag{28}$$

where $\mathbf{p} = m\,\dot{\mathbf{r}}$ is the translational momentum, $\boldsymbol{\pi} = \mathcal{I}\boldsymbol{\omega}$ is the angular momentum, $\mathbf{f}_r$ is the resultant force on the body, and $\mathbf{m}_r$ is the resultant couple. Integration of this form of the rigid body equation has been considered by Simo and Wong[10] and also used in the context of rigid-flexible systems by Chen.[26] We note that in the absense of external loadings that

$$\mathbf{p} = Constant \quad \text{and} \quad \boldsymbol{\pi} = Constant \tag{29}$$

and, thus, defines conservation of momentum properties for a rigid body.

For situations in which multiple rigid bodies are present, the conservation of momentum implies

$$\sum_a \mathbf{p}^{(a)} = Constant \quad \text{and} \quad \sum_a \left(\boldsymbol{\pi}^{(a)} + \mathbf{r}^{(a)} \times \mathbf{p}^{(a)} \right) = Constant \tag{30}$$

in which a denotes each rigid body number. Conservation of kinetic energy then requires

$$KE = \frac{1}{2} \sum_a \left[m^{(a)}\, (\mathbf{r}^{(a)})^T \mathbf{r}^{(a)} + (\boldsymbol{\omega}^{(a)})^T \mathcal{I}^{(a)}\, \boldsymbol{\omega}^{(a)} \right] = Constant \tag{31}$$

In developing discrete models for rigid-flexible bodies in terms of translations and rotations it is necessary to find consistent numerical time integration procedures. Failure to have consistency between the discrete translations and rotation updates can lead to anomalous results as shown by Jelenic and Crisfield for rods.[27] One way to avoid such difficulties is to construct a formulation in terms of translation parameters only. For shell formulations such a construction has been developed by Ramm *et al.*[28, 29, 30] and Betsch *et al.*.[31] For rigid body dynamics the enforcement of the constraint given by Eq. (11) can be achieved discretely.[24]

2.3 Rigid bodies using translation parameters only

If we initially represent the rigid body in terms of a simplex finite element (i.e., a 3-node triangle in two dimensions or a 4-node tetrahedron in three dimensions) which is given by the isoparametric representation in terms of natural coordinates L_α as[32, 33]

$$\mathbf{X} = \sum_{\alpha=1}^{Nel} L_\alpha \breve{\mathbf{X}}_\alpha \tag{32}$$

and

$$\mathbf{x} = \sum_{\alpha=1}^{Nel} L_\alpha \breve{\mathbf{x}}_\alpha \tag{33}$$

in which $\breve{\mathbf{X}}_\alpha$ and $\breve{\mathbf{x}}_\alpha$ are positions of nodes in the reference and deformed coordinates, respectively, and Nel is the number of nodes required to describe the simplex (i.e., 3 or 4). The natural coordinates in this form are not all independent and are related through the constraint[32]

$$\sum_{\alpha=1}^{Nel} L_\alpha = 1 \tag{34}$$

A rigid body form is achieved by constraining the length of the edges of the simplex to their original length. Thus, the problem reduces to imposing a set of constraints

$$C_k = \frac{1}{2}\left[(\breve{\mathbf{x}}_\mu - \breve{\mathbf{x}}_\nu)^T(\breve{\mathbf{x}}_\mu - \breve{\mathbf{x}}_\nu) - (\breve{\mathbf{X}}_\mu - \breve{\mathbf{X}}_\nu)^T(\breve{\mathbf{X}}_\mu - \breve{\mathbf{X}}_\nu)\right] = 0 \tag{35}$$

in which the points μ and ν represent the end points of an edge to the simplex element and k is the edge number. Application of these constrains ensures that $\mathbf{E}$ is zero throughout the entire rigid body and, thus, Eq. (33) now describes a rigid body motion.

For each rigid body we may now write the equations of motion in the weak form

$$\delta\Pi = \int_\Omega \delta\mathbf{U}^T \rho_0 \, \dot{\mathbf{V}} \, \mathrm{d}\Omega + \sum_k \delta\lambda_k \, C_k + \sum_k \delta C_k \, \lambda_k - \delta\Pi_{ext} = 0 \tag{36}$$

where λ_k is a Lagrange multiplier and $\delta\lambda_k$ its variation.

The momentum for each master node on the simplex of a rigid body a is given by

$$\breve{\mathbf{p}}_\alpha^{(a)} = \mathbf{M}_{\alpha\beta}^{(a)} \, \mathbf{V}\beta^{(a)} \tag{37}$$

Conservation of the total linear momentum thus requires

$$\sum_a \left[\sum_\alpha \breve{\mathbf{p}}_\alpha^{(a)}\right] = Constant \tag{38}$$

similarly, the conservation of angular momentum requires

$$\sum_a \left[\breve{\mathbf{x}}_\alpha^{(a)} \times \breve{\mathbf{p}}_\alpha^{(a)} \right] = Constant \tag{39}$$

The kinetic energy for a system of rigid bodies is given by

$$KE = \frac{1}{2} \sum_a (\breve{\mathbf{V}}_\alpha^{(a)})^T \breve{\mathbf{p}}_\alpha^{(a)} = Constant \tag{40}$$

We note that each of these forms is identical to that for a typical finite element system if we substitute nodal quantities for the finite element for each of the nodal quantities of the master simplex element.

3 Discrete equations for rigid bodies

A time discretized system for the rigid body may now be constructed. In the present work we use an energy-momentum conserving scheme as introduced by Simo and Wong[10] and used successfully for rigid body analyses in terms of the constraint form Eq. (35) by Taylor and Chen[34] and Chen.[26] For each rigid body we may write the discrete weak form as

$$\delta\Pi = \int_\Omega \delta\mathbf{U}^T \rho_0 \, \dot{\mathbf{V}}^{(n+1/2)} \, \mathrm{d}\Omega + \sum_k \delta\lambda_k \, C_k^{(n+1)} + \sum_k \delta C_k^{(n+1/2)} \, \lambda_k^{(n+1)} - \delta\Pi_{ext}^{(n+1/2)} = 0 \tag{41}$$

where $(\cdot)^{(n)}$ represents the discrete value of the quantity evaluated at time t_n. The variation of the constraint Eq. (35) is given by

$$\delta C_k^{(n+1/2)} = (\delta\breve{\mathbf{U}}_\mu - \delta\breve{\mathbf{U}}_\nu)^T (\breve{\mathbf{x}}_\mu^{(n+1/2)} - \breve{\mathbf{x}}_\nu^{(n+1/2)}) \tag{42}$$

In the above we note that the constraints are satisfied at the discrete times t_{n+1} whereas other quantities are evaluated at the mid-time interval $t_{n+1/2}$. The proof of satisfaction of momentum and energy conservation using this structure is given by Chen.[26]

Introducing now the isoparametric expansions given by Eqs (32) and (33) and noting that nodal displacements on the simplex may be introduced as

$$\breve{\mathbf{x}}_\alpha = \breve{\mathbf{X}}_\alpha + \breve{\mathbf{U}}_\alpha \tag{43}$$

we can write the discrete form as

$$\begin{aligned} \delta\breve{\mathbf{U}}_\alpha^T \left[\int_\Omega L_\alpha \, \rho_0 \, L_\beta \, \mathrm{d}\Omega \right] \dot{\breve{\mathbf{V}}}_\beta^{(n+1/2)} + \sum_k \delta\lambda_k \, C_k^{(n+1)} \\ + \sum_k (\delta\breve{\mathbf{U}}_\mu - \delta\breve{\mathbf{U}}_\nu)^T (\breve{\mathbf{x}}_\mu^{(n+1/2)} - \breve{\mathbf{x}}_\nu^{(n+1/2)}) \, \lambda_k^{(n+1)} = \delta\breve{\mathbf{U}}_\alpha^T \, \mathbf{F}^{(n+1/2)} \end{aligned} \tag{44}$$

in which $\mathbf{F}_\alpha^{(n+1/2)}$ are the discrete forces from body force and external loading effects.

The discrete form of the momentum equations are now given by

$$\mathbf{M}_{\alpha\beta}\,\dot{\breve{\mathbf{V}}}_{\beta}^{(n+1/2)} + \mathbf{G}_{\alpha k}^{(n+1/2)}\,\lambda_k^{(n+1)} = \mathbf{F}_{\alpha}^{(n+1/2)} \tag{45}$$

and the constraint equations by

$$C_k(\mathbf{U}^{(n+1)}) = 0 \tag{46}$$

The mass matrix is computed from

$$\mathbf{M}_{\alpha\beta} = \int_{\Omega} L_\alpha\,\rho_0\,L_\beta\,\mathrm{d}\Omega\,\mathbf{I} \tag{47}$$

with the constraint C_k is given by Eq. (2.11) and

$$\delta\breve{\mathbf{U}}_{\alpha}^{T}\,\mathbf{G}_{\alpha k}^{(n+1/2)} = (\delta\breve{\mathbf{U}}_{\mu} - \delta\breve{\mathbf{U}}_{\nu})^{T}(\breve{\mathbf{x}}_{\mu}^{(n+1/2)} - \breve{\mathbf{x}}_{\nu}^{(n+1/2)}) \tag{48}$$

for each constraint.

A Newton-Raphson scheme may be adopted to solve these nonlinear equations. Linearizing the momentum equation we obtain

$$\mathbf{M}_{\alpha\beta}\,d\dot{\breve{\mathbf{V}}}_{\beta}^{(n+1/2)} + \mathbf{K}_{\alpha\beta}\,d\breve{\mathbf{U}}_{\beta}^{(n+1/2)} + \mathbf{G}_{\alpha k}^{(n+1/2)}\,d\lambda_k^{(n+1)} = \mathbf{R}_{\alpha}^{(n+1/2)} \tag{49}$$

where $d\mathbf{U}$, $d\dot{\mathbf{V}}$ and $d\lambda$ denote incremental quantities, $\mathbf{K}_{\alpha\beta}$ is a *geometric* stiffness arising from the linearization of the variation of the constraints that may be expressed as

$$\delta\breve{\mathbf{U}}_{\alpha}^{T}\,\mathbf{K}_{\alpha\beta}\,d\breve{\mathbf{U}}_{\beta}^{(n+1/2)} = \lambda_k\,(\delta\breve{\mathbf{U}}_{\mu} - \delta\breve{\mathbf{U}}_{\nu})^{T}(\,d\breve{\mathbf{U}}_{\mu}^{(n+1/2)} - d\breve{\mathbf{U}}_{\mu}^{(n+1/2)}) \tag{50}$$

and

$$\mathbf{R}_{\alpha} = \mathbf{F}_{\alpha}^{(n+1/2)} - \mathbf{M}_{\alpha\beta}\,\dot{\breve{\mathbf{V}}}_{\beta}^{(n+1/2)} - \mathbf{G}_{\alpha k}^{(n+1/2)}\,\lambda_k^{(n+1)} \tag{51}$$

is a residual for each iteration of the solution process. Similarly, the linearization of constraints gives the relations

$$(\mathbf{G}_{\beta k}^{(n+1)})^{T}\,d\breve{\mathbf{U}}_{\beta}^{(n+1)} = r_k^{(n+1)} \tag{52}$$

where r_k is a residual for the constraint equation (46).

We next introduce a discrete time solution process and show that increments at time $t_{n+1/2}$ and t_{n+1} are linearly related and that the increment in the velocity rate may be expressed in terms of an increment of the displacements. Accordingly, in this case we will obtain a set of equations which may be expressed entirely in increments of displacements and Lagrange multipliers at t_{n+1}.

3.1 Time discrete solutions for the rigid body – energy-momentum conservation

A time discrete form is introduced in which the conservation of linear and angular momentum is ensured. In addition, when combined with flexible bodies with fully elastic behavior, energy is conserved. The time integration procedure to be used for the rigid body is based on the energy-momentum conserving schemes used successfully by Simo *et al.* to integrate rigid body motions[10], for flexible systems composed of solids and rods[40, 41, 42, 43, 44, 35] and for combined rigid-flexible systems.[34, 26, 24] The discretization proceeds by approximation of the translational acceleration by

$$\dot{\breve{\mathbf{V}}}^{(n+1/2)} = \frac{1}{\Delta t}\left(\breve{\mathbf{V}}^{(n+1)} - \breve{\mathbf{V}}^{(n)}\right) \tag{53}$$

where $\Delta t = t_{n+1} - t_n$. The displacement is then advanced using the average velocity as

$$\breve{\mathbf{U}}^{(n+1)} = \breve{\mathbf{U}}^{(n)} + \frac{1}{2}\Delta t\,\left(\breve{\mathbf{V}}^{n+1} + \breve{\mathbf{V}}^{(n)}\right) \tag{54}$$

so that the deformed configuration is given in ters of nodal quantities fo the simplex as

$$\breve{\mathbf{x}}^{(n+1)} = \breve{\mathbf{X}} + \breve{\mathbf{U}}^{(n+1)} \tag{55}$$

The mid-point position is then given by interpolation as

$$\breve{\mathbf{x}}^{(n+1/2)} = \frac{1}{2}\left(\breve{\mathbf{x}}^{(n)} + \breve{\mathbf{x}}^{(n+1)}\right) \tag{56}$$

Using the above formulae, the residual for the discrete momentum equation may be written as

$$\mathbf{R}_{\alpha}^{(n+1/2)} = \mathbf{F}_{\alpha}^{(n+1/2)} - \frac{1}{\Delta t}\mathbf{M}_{\alpha\beta}\left(\breve{\mathbf{V}}_{\beta}^{(n+1)} - \breve{\mathbf{V}}_{\beta}^{(n)}\right) - \mathbf{G}_{\alpha k}^{(n+1/2)}\,\lambda_{k}^{(n+1)} = \mathbf{0} \tag{57}$$

and the residual for the constraint equation as

$$r_k = -\,C_k(\mathbf{U}^{(n+1)}) = 0 \tag{58}$$

Using Eqs (53) to (56) the increments in the displacement may be related to the increment of the velocity by

$$d\breve{\mathbf{x}}^{(n+1)} = d\breve{\mathbf{U}}^{(n+1)} = \frac{1}{2}\Delta t\, d\breve{\mathbf{V}}^{(n+1)} \tag{59}$$

and the mid-point solution values by

$$\begin{aligned} d\breve{\mathbf{x}}^{(n+1/2)} &= \tfrac{1}{2}\, d\breve{\mathbf{x}}^{(n+1)} \\ d\breve{\mathbf{U}}^{(n+1/2)} &= \tfrac{1}{2}\, d\breve{\mathbf{U}}^{(n+1)} \end{aligned} \tag{60}$$

The linearization of Eqs (57) and (58) may now be written as[2]

$$\left[\begin{array}{cc} \frac{2}{\Delta t^2}\mathbf{M}_{\alpha\beta} + \frac{1}{2}\mathbf{K}_{\alpha\beta} & \mathbf{G}_{\alpha k}^{(n+1/2)} \\ (\mathbf{G}_{\beta l}^{(n+1)})^T & \mathbf{0} \end{array} \right] \left\{ \begin{array}{c} d\breve{\mathbf{U}}_{\beta}^{(n+1)} \\ d\lambda_k^{(n+1)} \end{array} \right\} = \left\{ \begin{array}{c} \mathbf{R}_{\alpha}^{(n+1/2)} \\ r_l^{(n+1)} \end{array} \right\} \tag{61}$$

The solution is then advanced using

$$\left\{ \begin{array}{c} \breve{\mathbf{U}}_{\beta}^{(n+1)} \\ d\lambda_k^{(n+1)} \end{array} \right\} \leftarrow \left\{ \begin{array}{c} \breve{\mathbf{U}}_{\beta}^{(n+1)} \\ \lambda_k^{(n+1)} \end{array} \right\} + \left\{ \begin{array}{c} d\breve{\mathbf{U}}_{\beta}^{(n+1)} \\ d\lambda_k^{(n+1)} \end{array} \right\} \tag{62}$$

and iteration continues until the residuals are zero to within a specified tolerance.

As is common in energy-momentum algorithms, the above set of equations is unsymmetric. The asymmetry appears only through the manner in which the rigid constraint C_k must be introduced in order to conserve energy. In the case of individual rigid bodies this fact is not too severe since in two dimensions the $\mathbf{M}_{\alpha\beta}$ and $\mathbf{K}_{\alpha\beta}$ arrays are given as 6×6 matrices and $\mathbf{G}_{\alpha k}$ is a 6×3 matrix (in three dimensions they are 12×12 and 12×6, respectively). However, when combined with hyperelastic flexible bodies which are also treated by an energy-momentum conserving scheme further asymmetry will exist with respect to the tangent stiffness part which now is much larger in general.[40, 41, 45, 42]

A perturbed lagrangian scheme may be introduced to eliminate the Lagrange multipliers locally for each rigid body. Accordingly, we modify Eq. (61) to read

$$\left[\begin{array}{cc} \frac{2}{\Delta t^2}\mathbf{M}_{\alpha\beta} + \frac{1}{2}\mathbf{K}_{\alpha\beta} & \mathbf{G}_{\alpha k}^{(n+1/2)} \\ (\mathbf{G}_{\beta l}^{(n+1)})^T & -\frac{1}{\eta}\delta_{lk} \end{array} \right] \left\{ \begin{array}{c} d\breve{\mathbf{U}}_{\beta}^{(n+1)} \\ d\lambda_k^{(n+1)} \end{array} \right\} = \left\{ \begin{array}{c} \mathbf{R}_{\alpha}^{(n+1/2)} \\ r_l^{(n+1)} \end{array} \right\} \tag{63}$$

in which δ_{lk} is a Kronecker delta and η is the augmented lagrangian 'penalty' parameter. We then perform static condensation[46] using the second row to obtain the form

$$\left[\frac{2}{\Delta t^2}\mathbf{M}_{\alpha\beta} + \frac{1}{2}\mathbf{K}_{\alpha\beta} + \eta\, \mathbf{G}_{\alpha k}^{(n+1/2)} (\mathbf{G}_{\beta k}^{(n+1)})^T \right] d\breve{\mathbf{U}}_{\beta}^{(n+1)} = \mathbf{R}_{\alpha}^{(n+1/2)} + (\mathbf{G}_{\beta l}^{(n+1)})^T r_l^{(n+1)} \tag{64}$$

After convergence of the Newton-Raphson algorithm each Lagrange multiplier may be updated using the simple Uzawa formula[47, 33]

$$\lambda_k \leftarrow \lambda_k + \eta\, (\mathbf{G}_{\beta k}^{(n+1)})^T\, d\breve{\mathbf{U}}_{\beta}^{(n+1)} \tag{65}$$

and another pass through the iteration steps performed. This involves an extra iteration loop which may be used to satisfy the rigid constraints to a specified tolerance. An asymmetry of the tangent matrix is still encountered as indicated by the coefficient matrix in Eq. (64) but final matrices involved are of size $\mathbf{M}$ only. In results presented later the Lagrange multiplier form is used exclusively.

[2]Note that for simplicity in notation we do not include an iteration index.

4 Flexible elements – no rotations parameters

4.1 Continuum elements – energy-momentum conserving

Continuum elements which satisfy discrete energy-momentum conservation for hyperelastic formulations may be developed from Eq. (7). Here, we restrict attention to the case of a St. Venant-Kirchhoff material where, for simplicity, the stress-strain behavior is given in indicial form by

$$S_{IJ} = C_{IJKL}\, E_{KL} \tag{66}$$

in which C_{IJKL} are the elastic moduli. Generalizations to the development may be constructed by following the procedures summarized by Gonzalez.[35] The energy-moment algorithm for a flexible body may be expressed as

$$\frac{1}{\Delta t}\,\delta\mathbf{U}_\alpha^T\,\mathbf{M}_{\alpha\beta}\left[\mathbf{V}_\beta^{(n+1)} - \mathbf{V}_\beta^{(n)}\right] + \int_\Omega \delta\mathbf{E}^{(n+1/2)}\mathbf{S}^{(n+1/2)}\,\mathrm{d}\Omega = \delta\mathbf{U}_\alpha^T\,\mathbf{F}_\alpha^{(n+1/2)} \tag{67}$$

where, again in index form

$$\delta E_{IJ}^{(n+1/2)} = \delta F_{iI}\,F_{iJ}^{(n+1/2)} + \delta F_{iJ}\,F_{iI}^{(n+1/2)} \tag{68}$$

and

$$S_{IJ}^{(n+1/2)} = C_{IJKL}\left[\frac{1}{2}\left(E_{KL}^{(n)} + E_{KL}^{(n+1)}\right)\right] \tag{69}$$

The development of a finite element from this form may now be constructed by introducing isoparametric interpolations for the position and displacements as

$$\mathbf{X} = \sum_\alpha^{Nel} N_\alpha(\boldsymbol{\xi})\,\tilde{\mathbf{X}}_\alpha \tag{70}$$

and

$$\mathbf{U}^{(n)} = \sum_\alpha^{Nel} N_\alpha(\boldsymbol{\xi})\,\tilde{\mathbf{U}}_\alpha^{(n)} \tag{71}$$

in which $\boldsymbol{\xi}$ are natural coordinates, N_α are shape functions, and $\tilde{\mathbf{X}}_\alpha$, $\tilde{\mathbf{U}}_\alpha^{(n)}$ are nodal quantities. A typical 4-node element of rectangular form is shown in Fig. 3.

4.2 Structural elements – energy-momentum conserving

The above form is classical as far as the finite element treatment and energy-momentum conservation is concerned. However, the development of structural element types (e.g., rods or shells) in which no rotation parameters exist is not typical. Formulations for small deformation behavior of thin plates in which no rotation parameters exist was developed by

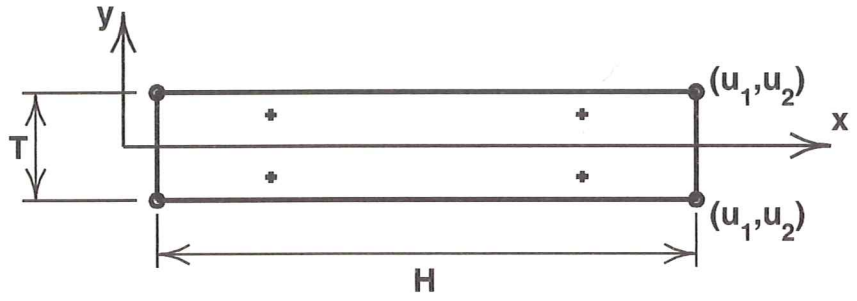

Figure 3: Solid element: + denotes Gauss point locations

Nay and Utku in 1972.[36] More recently Oñate and co-workers have developed thin plate and shell elements which have only translation degrees of freedom.[37, 38, 39] Such forms can be extended to large displacement-small strain applications using updated or corotational forms. Also recently, the development of shell elements which have no rotation parameters has been presented by Ramm and co-workers and Stein and co-workers as already cited above. These latter works are valid for both small and large displacement formulations.

Here we adopt a simple form of that used for large deformation of shells to analyze two-dimensional rod (beam) applications. In the form adopted, the nodal displacements for the isoparametric 4-node element described above are transformed to mid-surface displacements and top surface incremental displacements as shown in Fig. 4

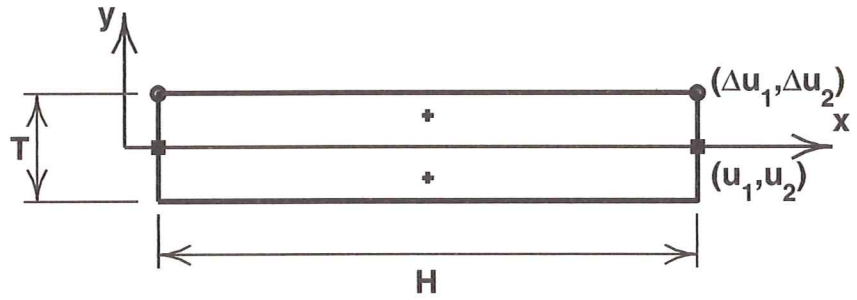

Figure 4: Beam element without rotation parameters: + denotes Gauss point location

In addition, it is well known that the 'two-node' beam formulation will experience shear locking unless reduced integration is used to compute the stiffness matrix. Accordingly, as also indicated in Fig. 4 we also use a reduced integration along the beam axis direction to compute the stress residual and stiffness terms. This form permits the consideration of general constitutive behavior without further modification only if no coupling exists between the beam direction normal stresses and the through thickness normal stress. Accordingly, we consider only forms for which C_{IJKL} is diagonal (e.g., Poisson ratio is zero). Enhanced strain forms can be introduced to remove this restriction.[28, 31]

The above form is very easy to implement and leads to good performance for the problems considered in this study.

5 Construction of the mass for rigid bodies

In Section 3 we expressed the mass for the rigid body as

$$\mathbf{M}_{\alpha\beta} = \int_{\Omega} L_\alpha \, \rho_0 \, L_\beta \, \mathrm{d}\Omega \, \mathbf{I} \tag{72}$$

where L_α are the natural coordinates for the simplex master element.

Here, we consider the case where a rigid body is described in terms of a finite element representation and is to be constrained to the simplex as shown in Figure 5. We assume that

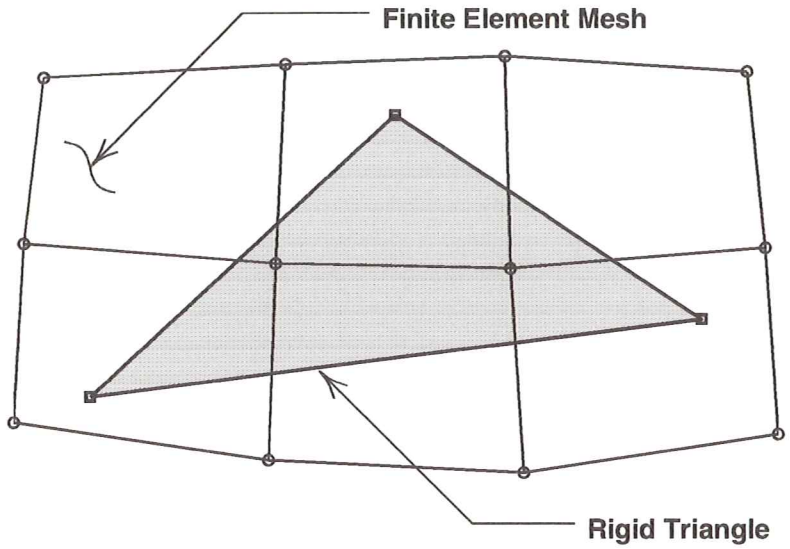

Figure 5: Finite element representation of a rigid body

the mass matrix is available for each finite element and is given by $\mathbf{m}^{(e)}_{\mu\nu}$ in which μ and ν denote the node numbers in the finite element mesh. Accordingly, we can relate the inertial forces for each form as

$$\delta\breve{\mathbf{U}}^T_\alpha \, \mathbf{M}_{\alpha\beta} \ddot{\breve{\mathbf{x}}}_\beta = \sum_e \delta\tilde{\mathbf{U}}^T_\mu \, \mathbf{m}^{(e)}_{\mu\nu} \, \ddot{\tilde{\mathbf{x}}}_\nu \tag{73}$$

to complete the transformation it only remains to express the virtual displacements and accelerations of a node in terms of those on the simplex. Using Eqs (32), (33) and (43) we obtain

$$\delta\tilde{\mathbf{U}}_\mu = L^\mu_\alpha \, \delta\breve{\mathbf{U}}_\alpha \tag{74}$$

and

$$\ddot{\tilde{\mathbf{x}}}_\mu = L^\mu_\alpha \, \ddot{\breve{\mathbf{x}}}_\alpha \tag{75}$$

in which L^μ_α denotes the natural coordinates evaluated at the μ node. These are determined by solving the linear equations relating the cartesian coordinates to their natural coordinates [e.g., Eq. (32)] and considering the constraint given by Eq. (34). For example, in two dimensions we solve the set of equations for node μ which are given by

$$\left\{ \begin{array}{c} 1 \\ (\tilde{X}_1)_\mu \\ (\tilde{X}_2)_\mu \end{array} \right\} = \left[\begin{array}{ccc} 1 & 1 & 1 \\ (\breve{X}_1)_1 & (\breve{X}_1)_2 & (\breve{X}_1)_3 \\ (\breve{X}_2)_1 & (\breve{X}_2)_2 & (\breve{X}_2)_3 \end{array} \right] \left\{ \begin{array}{c} L^\mu_1 \\ L^\mu_2 \\ L^\mu_3 \end{array} \right\} \tag{76}$$

In the above $(\tilde{X}_1)_\mu$ and $(\tilde{X}_2)_\mu$ denote the cartesian coordinates of node μ and $(\breve{X}_1)_1$, $(\breve{X}_2)_1$, etc. the cartesian coordinates of the simplex used to describe the motion of the rigid body.

Introducing the solution for the natural coordinates and using Eqs (73), (74) and (75) we may express the mass [using Eq. (72)] as

$$\mathbf{M}_{\alpha\beta} = \sum_e L^\mu_\alpha \, \mathbf{m}^{(e)}_{\mu\nu} \, L^\nu_\beta \tag{77}$$

in which summation over repeated indices is implied.

6 Rigid-flexible interface and joint descriptions

The analysis of systems composed of rigid and flexible parts requires the treatment of two connection processes. In the most basic form a rigid body many be 'bonded' directly to a flexible body along an interface as shown in Fig. 6. Alternatively, we have situations in which two rigid bodies are constrained to move relative to one another in a specific manner. This latter behavior requires introduction of constraint conditions which are commonly referred to as *joints*. Here we describe briefly the treatment of both types of constrained conditions.

6.1 Rigid-flexible interface treatment

The motion of nodes on the flexible body which lie on the interface of a rigid body, must satisfy the motion constraint given by Eq. (32), assuming such already satisfies the set of constraints given by Eq. (35). Accordingly, these nodes have the behavior

$$\tilde{\mathbf{x}}_\mu = \sum_\alpha L^\mu_\alpha \, \breve{\mathbf{x}}_\alpha \tag{78}$$

or

$$\tilde{\mathbf{U}}_\mu = \sum_\alpha L^\mu_\alpha \, \breve{\mathbf{U}}_\alpha \tag{79}$$

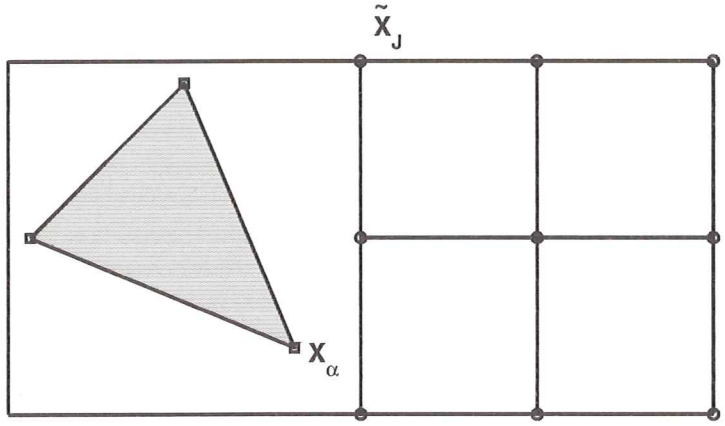

Figure 6: Rigid-flexible interface treatment

with a similar computation procedure as defined in Eq. (76).

Using these relations the residual and tangent matrices for a flexible element node on a rigid interface is transformed to be expressed in terms of the degrees of freedom on the master element. In this set of transformation one need not be concerned with the rigid body constraints as they only serve to ensure that the quantities $\breve{\mathbf{x}}_\alpha$, etc. are indeed moving as a rigid body. The equations to be transformed may be expressed as

$$\delta\tilde{\mathbf{U}}_\mu^T \, \mathbf{K}^\star_{\mu\nu} \, d\tilde{\mathbf{U}}_\nu = \delta\tilde{\mathbf{U}}_\mu^T \, \mathbf{R}_\mu \tag{80}$$

in which $\mathbf{R}_\mu$ is the element residual for node μ and $\mathbf{K}^\star_{\mu\nu}$ is the total tangent matrix from the flexible element and includes inertia, internal force and geometric stiffness parts. For the energy-momentum method it has the general form

$$\mathbf{K}^\star_{\mu\nu} = \frac{2}{\Delta t^2}\,\mathbf{m}^{(e)}_{\mu\nu} + \frac{1}{2}\left(\mathbf{k}^{(e)}_{\mu\nu}\big|_M + \mathbf{k}^{(e)}_{\mu\nu}\big|_G\right) \tag{81}$$

with $\mathbf{m}^{(e)}$ and $\mathbf{k}^{(e)}$ denoting the element mass and tangent stiffness quantities, respectively. Accordingly, for nodes on the rigid interface we perform the transformation as

$$\delta\breve{\mathbf{U}}_\alpha^T \left(\sum_{\nu_{flex}} L^\mu_\alpha \, \mathbf{K}^\star_{\mu\nu} \, d\tilde{\mathbf{U}}_\nu + \sum_{\nu_{rigid}} L^\mu_\alpha \, \mathbf{K}^\star_{\mu\nu} \, L^\nu_\beta \, d\breve{\mathbf{U}}_\beta \right) = \delta\breve{\mathbf{U}}_\alpha^T \, \left(L^\mu_\alpha \, \mathbf{R}_\mu\right) \tag{82}$$

similarly for each flexible node on which a node is attached to a rigid body we transform as

$$\delta\tilde{\mathbf{U}}_\mu^T \left(\sum_{\nu_{flex}} \mathbf{K}^\star_{\mu\nu} \, d\tilde{\mathbf{U}}_\nu + \sum_{\nu_{rigid}} \mathbf{K}^\star_{\mu\nu} \, L^\nu_\beta \, d\breve{\mathbf{U}}_\beta \right) = \delta\tilde{\mathbf{U}}_\mu^T \, \mathbf{R}_\mu \tag{83}$$

Thus, in matrix form, we have the transformed equations

$$\begin{bmatrix} L^{\mu}_{\alpha}\,\mathbf{K}^{\star}_{\mu\nu}\,L^{\nu}_{\beta} & L^{\mu}_{\alpha}\,\mathbf{K}^{\star}_{\mu\nu} \\ \mathbf{K}^{\star}_{\mu\nu}\,L^{\nu}_{\beta} & \mathbf{K}^{\star}_{\mu\nu} \end{bmatrix} \begin{Bmatrix} d\breve{\mathbf{U}}_{\beta} \\ d\tilde{\mathbf{U}}_{\nu} \end{Bmatrix} = \begin{Bmatrix} L^{\mu}_{\alpha}\,\mathbf{R}_{\mu} \\ \mathbf{R}_{\mu} \end{Bmatrix} \tag{84}$$

in which the residual in the first row is added to ther residual of the rigid body master node and the first term in the first row of the tangent matrix is added to the appropriate term in the rigid body tangent matrix. This step follow exactly the steps performed to combine flexible elements with rigid bodies described by the rigid motion described by eq. (11) as described by Taylor and Chen[34] and Chen.[26]

The computations for incremental displacements are only slightly more complicated as in this case we have the relation that the position here is given by

$$\mathbf{x}(\tilde{\mathbf{X}}_{\mu} + \Delta\tilde{\mathbf{X}}_{\mu}) = \tilde{\mathbf{x}}_{\mu} + \Delta\tilde{\mathbf{x}}_{\mu} \tag{85}$$

or

$$\mathbf{U}(\tilde{\mathbf{X}}_{\mu} + \Delta\tilde{\mathbf{X}}_{\mu}) = \tilde{\mathbf{U}}_{\mu} + \Delta\tilde{\mathbf{U}}_{\mu} \tag{86}$$

Thus, a similar process as that described above also is performed for each node which has degrees of freedom defined by such incremental quantities.

6.2 Multi-body coupling by joints

Often it is desirable to have two (or more) rigid bodies connected in some specified manner. For example, in Fig. 7 we show a disk connected to an arm. Both are treated as rigid bodies but it is desired to have the disk connected to the arm in such a way that it can rotate freely about the axis normal to the page. This type of motion is characteristic of many rotating machine connections and it, as well as many other types of connections are encountered in the study of rigid body motions.[6, 48] An interconnection of this type is commonly referred to as a *joint*. In quite general terms joints may be constructed by a combination of two types of simple constraints: *translational constraints* and *rotational constraints*.

6.2.1 Translation constraints

The simplest type of joint is a spherical connection in which one body may freely rotate around the other but relative translation is prevented. Such a situation is shown in Fig. 7 where it is evident the spinning disk must stay attached to the rigid arm at its axle. Thus it may not translate relative to the arm in any direction (additional constraints are necessary to ensure it rotates only about the one axis – these are discussed in Section 6.2.2). If full translation constraint is imposed a simple relation may be introduced as

$$\mathbf{C}_j = \mathbf{x}_j^{(a)} - \mathbf{x}_j^{(b)} = \mathbf{0} \tag{87}$$

where a and b denote two rigid bodies. Thus, addition of the Lagrange multiplier constraint

$$\delta\Pi_j = \delta\boldsymbol{\lambda}_j^T \left[\mathbf{x}_j^{(a)} - \mathbf{x}_j^{(b)}\right] + \left[\delta\mathbf{x}_j^{(a)} - \delta\mathbf{x}_j^{(b)}\right]^T \boldsymbol{\lambda}_j \tag{88}$$

imposes the spherical joint condition. It is only necessary to define the location for the spherical joint in the reference configuration. Denoting this as $\mathbf{X}_j$ (which is common to the two bodies) and introducing the rigid motion yields a constraint in terms of the rigid body positions as

$$\begin{aligned} \delta\Pi_j &= \delta\boldsymbol{\lambda}_j^T \left[\mathbf{X}_j^{(a)} + \mathbf{U}_j^{(a)} - \mathbf{X}_j^{(b)} - \mathbf{U}_j^{(b)} \right] + \left[\delta\mathbf{U}_j^{(a)} - \delta\mathbf{U}_j^{(b)} \right]^T \boldsymbol{\lambda}_j \\ &= \delta\boldsymbol{\lambda}_j^T \left[\mathbf{U}_j^{(a)} - \mathbf{U}_j^{(b)} \right] + \left[\delta\mathbf{U}_j^{(a)} - \delta\mathbf{U}_j^{(b)} \right]^T \boldsymbol{\lambda}_j \end{aligned} \tag{89}$$

The variation and subsequent linearization of this relation yields the contribution to the residual and tangent matrix for each body, respectively. This is easily performed using relations given above.

If the translation constraint is restricted to be in one direction with respect to, say, body a it is necessary to track this direction and write the constraint accordingly. To accomplish this the specific direction of the body a in the reference configuration is required. This may be computed by defining two points in space $\mathbf{X}_1$ and $\mathbf{X}_2$ from which a unit vector $\mathbf{V}$ is defined by

$$\mathbf{V} = \frac{\mathbf{X}_2 - \mathbf{X}_1}{\mid \mathbf{X}_2 - \mathbf{X}_1 \mid} \tag{90}$$

The direction of this vector in the current configuration, $\mathbf{v}$, may be obtained using the displacements of the points. Accordingly,

$$\mathbf{v} = \frac{\mathbf{x}_2 - \mathbf{x}_1}{\mid \mathbf{x}_2 - \mathbf{x}_1 \mid} \tag{91}$$

where

$$\mathbf{x}_i = \mathbf{X}_i + \mathbf{U}_i \tag{92}$$

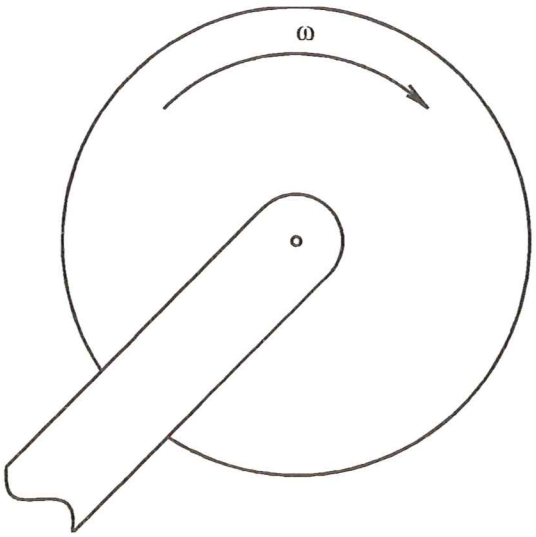

Figure 7: Spinning disk constrained by a joint to a rigid arm

A constraint can now be introduced into the variational problem as

$$\delta\Pi_j = \delta\lambda_j \, \mathbf{v}^T \left(\mathbf{x}_j^{(a)} - \mathbf{x}_j^{(b)} \right) + \left[\delta\mathbf{v}^T \left(\mathbf{x}_j^{(a)} - \mathbf{x}_j^{(b)} \right) + \mathbf{v}^T \left(\delta\mathbf{x}_j^{(a)} - \delta\mathbf{x}_j^{(b)} \right) \right] \lambda_j \qquad (93)$$

where, due to the fact there is only a single constraint direction the Lagrange multiplier is a scalar λ_j and, again, $\mathbf{X}_j$ denotes the reference position where the constraint is imposed.

The above constraints may also be imposed using a penalty function. The most direct form is to *perturb* each Lagrange multiplier form by a penalty term. Accordingly, for each constraint we write the variational problem as

$$\delta\Pi_j = \delta \left[\lambda_j \, C_j - \frac{1}{2\,k} \, \lambda_j^2 \right] \qquad (94)$$

where it is immediately obvious that the limit $k \to \infty$ yields exact satisfaction of the constraint. Use of a large k and performing the variation with respect to λ_j gives

$$\delta\lambda_j \left[C_j - \frac{1}{k} \, \lambda_j \right] = 0 \qquad (95)$$

which may be easily solved for the Lagrange multiplier as

$$\lambda_j = k \, C_j \qquad (96)$$

which when substituted back into Eq. (94) gives the classical form

$$\delta\Pi_j = \delta C_j \, k \, C_j \qquad (97)$$

An augmented lagrangian form is also possible following the procedures summarized above for treating the constraint on rigid body motion (see also [32]).

Implementation of the constraints is straight forward and follows the procedures introduced above to express points in terms of the degrees of freedom of the master simplex element (e.g., $\breve{\mathbf{U}}_\alpha$). It is immediately evident that when the constraint point is chosen at a node of the master element considerable simplification occurs and direct substitution of the nodal quantities $\breve{\mathbf{X}}_\alpha$ and $\breve{\mathbf{U}}_\alpha$ may be made. Thus, for example to introduce a spherical joint between two rigid bodies it is only necessary to place a node of the simplex for each body at the joint location and to assign to this node the same global node number in an analogous manner to connecting two normal finite elements at a node. This possibility is not available when using traditional translation ($\mathbf{r}$) and rotation parameters ($\mathbf{\Lambda}$) for rigid bodies, thus providing an advantage for the rotation free formulation.

6.2.2 Rotation constraints

A second kind of constraint that needs to be considered relates to rotations. We have already observed in Fig. 7 that the disk is free to rotate around only one axis. Accordingly, constraints must be imposed which limit this type of motion. This may be accomplished by constructing an orthogonal set of vectors $\mathbf{V}_I$ in the reference configuration as described by Eqs (90) to (92) and tracking their orientation in the deformed body.

A rotational constraint which imposes that axis i of body a remain perpendicular to axis j of body b may then be written as

$$(\mathbf{v}_i^{(a)})^T \mathbf{v}_j^{(b)} = \mathbf{V}_I^T \mathbf{V}_J = 0 \tag{98}$$

More general constraints on rotation may be imposed by satisfying orthogonality conditions between the two rigid bodies. These constraints (assuming that $\mathbf{V}_{(a)} = \mathbf{V}_{(b)}$ in the reference state) are given by conditions

$$C_k = (\mathbf{v}_i^{(a)})^T \mathbf{v}_i^{(b)} = 1 \tag{99}$$

or

$$C_k = (\mathbf{v}_i^{(a)})^T \mathbf{v}_j^{(b)} = 0 \tag{100}$$

Indeed, it is not necessary to use unit vectors if Eq. (99) is modified to

$$C_k = (\mathbf{v}_i^{(a)})^T \mathbf{v}_i^{(b)} = \mathbf{V}_j^T \mathbf{V}_j \tag{101}$$

again assuming that the vectors in the reference configuration are equal in the two bodies.

6.2.3 Example: Revolute joint

As an example, consider the situation shown for the disk in Fig. 7 and define the axis of rotation in the reference configuration by the cartesian coordinate unit vectors in the reference system $\mathbf{E}_I$ (i.e., $\mathbf{V}_I = \mathbf{E}_I$). If we let the disk be body a and the arm body b the set of constraints can be written as (where $\mathbf{v}_3$ is axis of rotation)

$$\mathbf{C}_j = \left\{ \begin{array}{c} \mathbf{x}^{(a)} - \mathbf{x}^{(c)} \\ (\mathbf{v}_1^{(a)})^T \mathbf{v}_3^{(b)} \\ (\mathbf{v}_2^{(a)})^T \mathbf{v}_3^{(b)} \end{array} \right\} = \mathbf{0} \tag{102}$$

and included in a formulation using a Lagrange multiplier form

$$\delta \Pi_j = \delta \boldsymbol{\lambda}_j^T \mathbf{C}_j + \delta \mathbf{C}_j \boldsymbol{\lambda}_j^T \tag{103}$$

The modifications to the finite element equations are obtained by appending the variation and linearization of Eq. (103) to the usual equilibrium equations. Here, in three dimensions, five Lagrange multipliers are involved to impose the three translational constraints (spherical joint) and the angle constraints for the rotating disk. The set of constraints is known as a *revolute* joint.[2].

6.2.4 Library of joints

Translational and rotational constraints may be combined in many forms to develop different types of constraints between rigid bodies. For the development it is necessary to have only the three types of constraints described above. Namely, the spherical joint, a single

translational constraint, and a single rotational constraint. Once these are available it is possible to combine them to form classical constraint joints and here the reader is referred to the literature for the many kinds commonly encountered.[2, 6, 9, 26]

The only situation that requires special mention is the case when a series of rigid bodies is connected together to form a *closed loop*. In this case the method given above can lead to situations in which some of the joints are redundundant. Using Lagrange multipliers this implies the resulting tangent matrix will be singular and, thus, one cannot obtain solutions. Here the penalty method provides a viable method to circumvent this problem. The penalty method introduces *elastic deformation* in the joints and in this way removes the singular problem. If necessary an augmented Lagrangian method can be used to keep the deformation in the joint within required small tolerances. An alternative to this is to extract the closed loop rigid equations from the problem and use singular valued decomposition[49] to identify the redundant equations. These may then be removed by constructing a pseudo-inverse for the tangent matrix of the closed loop. This method has been used successfully by Chen to solve single loop problems.[26]

7 Example solutions

7.1 Square block

Figure 8 shows a square block with side lengths of 6 units which is modeled by one 4-node quadrilateral finite element. The master simplex element is a triangle with sides of 3-units and is positioned as shown on the block. No boundary restraints are applied. The motion of the block is initiated by a pair of equal but opposite horizontal forces: A positive force at node 1 and a negative force at node 3 of the master triangle. The force rises linearly to a magnitude of 4 at time 2 and then decreases linearly to zero at time 4. The mass density of the block is 2 units. The block rotates uniformly after time 4 without loads, and thus should conserve both angular momentum and energy.

A solution to the problem is computed using (a) the energy-momentum scheme described in this work; (b) a generalized mid-point scheme in which constraints are imposed with constraints and $\mathbf{G}$ matrices given at the mid-time step; and (c) a generalized mid-point scheme in which the constraints and $\mathbf{G}$ matrices are imposed at the end of each time step (i.e., at t_{n+1}). For this problem each of the integration schemes treats the inertial terms in an identical manner and, thus, the only difference is the manner of imposing constraints.

Figure 9 shows the angular momentum behavior and the need to satisfy constraints at the time mid-step is readily apparent. Satisfaction at the end of the time step by (c) leads to a decrease in angular momentum.

Figure 10 shows the behavior of energy and here it is clearly evident that the mid-point scheme (b) which satisfies the constraint at the time mid-step is unstable, with the solution becoming unbounded around time 150. The satisfaction of the constraint at the end of the step by method (c) leads to loss of energy, and eventually the block will cease to rotate. The energy-momentum conserving scheme is seen to behave properly: conserving both the angular momentum and the energy.

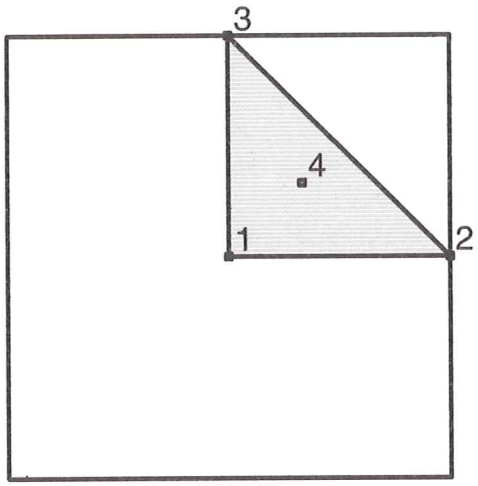

Figure 8: Square block with triangular master element.

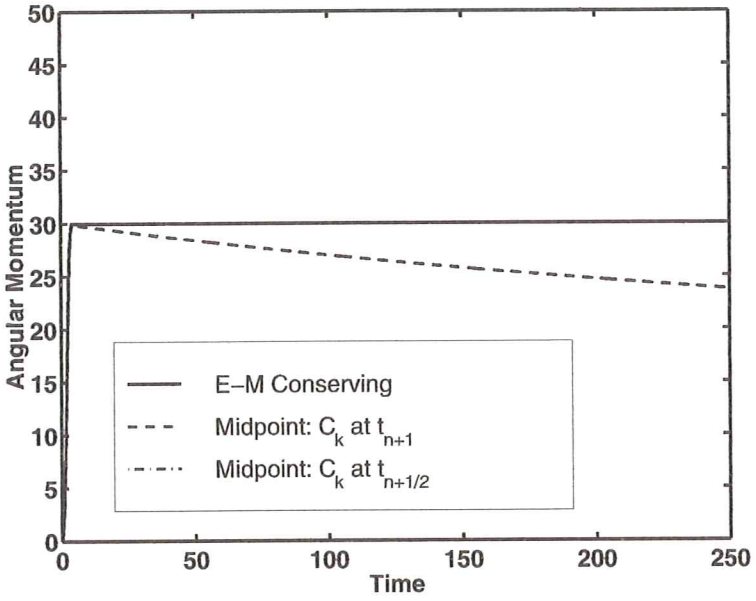

Figure 9: Square block: Angular momentum behavior.

7.2 Circular disk with flexible beam

As a second example we consider the problem of a circular disk with an attached flexible beam. The configuration of the system in its initial state is shown in Fig. 11. The radius of the disk is 3 units and the master triangle is imbedded as shown. The beam is attached to the right in an initial horizontal position as shown, and has length 10 units and depth 0.1 units and, thus, the beam is quite thin. The density of the rigid body is 0.2 units and

that for the beam is 2.0 units. The beam is modeled by a St. Venant-Kirchhoff material with C_{IJKL} expressed by a modulus, E, of 100,000 and a Poisson ratio, ν, of 0. The body is completely unrestrained and is set in free motion with a loading as described in the previous example.

A solution is constructed using the energy-momentum conserving algorithm described above with a uniform time step size of 0.5 units. A plot of the angular momentum of the system is shown in Fig. 12 and is clearly conserved throughout the free motion. In Fig. 13 a plot of the kinetic energy, stored energy in the flexible beam, and total energy is presented. Again, it is evident that the total energy is conserved during free motion. In Fig. 14 we show the behavior of the vertical displacement of each of the nodes used to describe the master simplex element. In particular, it is noted that the vibration of the beam causes an oscillation of the center of the rigid disk. Finally, in Fig. 15 we show a cartoon of the deformed positions for several of the times during the first two revolutions in the solution. Here it is seen that the beam undergoes large oscillations while rotating about the rigid disk.

7.3 Two blocks with revolute joint

The behavior of multiple rigid bodies requires the introduction of interconnections, generally called *joints*, to model the desired interactions. In the case of bodies modeled by the parent simplex use of such joints can be partially avoided by placing the nodes of the simplex at locations where a joint is needed. To demonstrate such situations we consider the simple problem of two square blocks which are interconnected by a revolute joint at the common

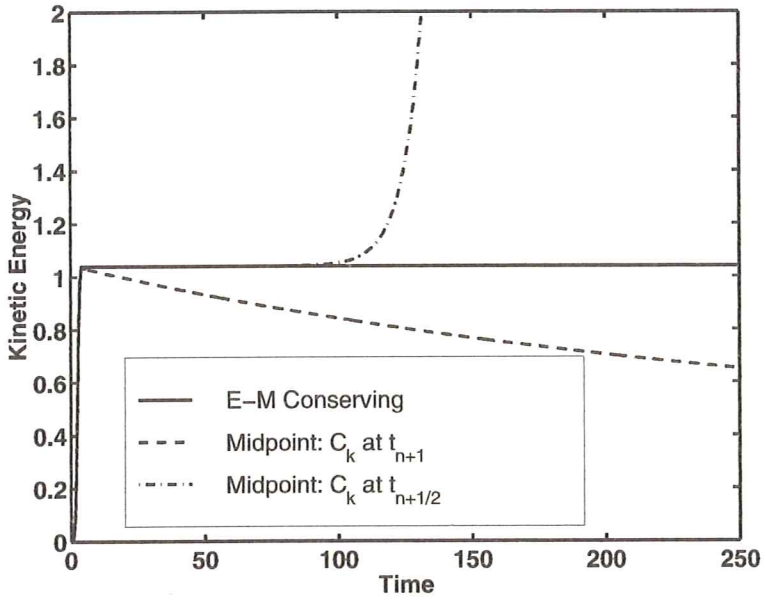

Figure 10: Square block: Kinetic energy behavior.

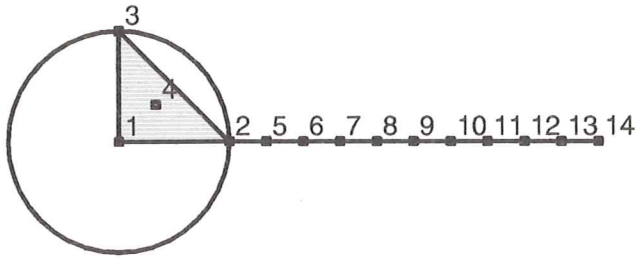

Figure 11: Circular disk with flexible beam attached. Initial state.

corner as indicated in Fig. 16 In the case of a two-dimensional problem such revolute joint also defines a spherical joint since the blocks cannot displace out of plane. By placing a node at the location of the 'joint' the interconnection may be accomplished without addition of constraints – one merely assigns the same node number to the common node, as indicated in Fig. 16. This expedient is far simpler than that needed for a formulation in terms of the center of mass motion with an added orthogonal rotation [viz.[[q. (12] and indeed it is possible to have three such revolute joints on a single rigid body in two dimensions (provided they are not all on a straight line). Of course if more are added it is then necessary to add a joint constraint set to represent the interconnection as described in Section 6.2. Further, if other types of joints are used it is necessary to specify the required constraints explicitly.

For the two block form we excite the problem by forces applied to nodes 2,3, and 5 in the same manner as in the previous two problems. The forces at nodes 3 and 5 have equal components in the positive x and y directions and node 2 has twice these forces in the

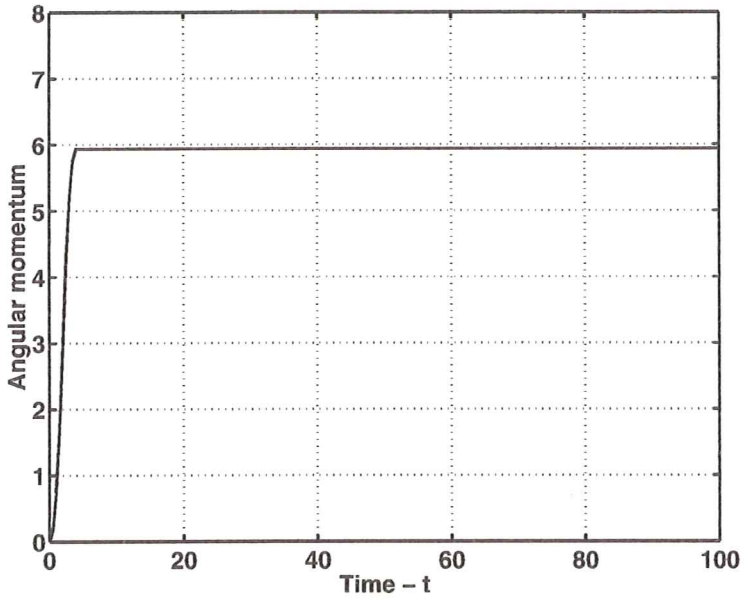

Figure 12: Circular disk with flexible beam attached. Angular momentum.

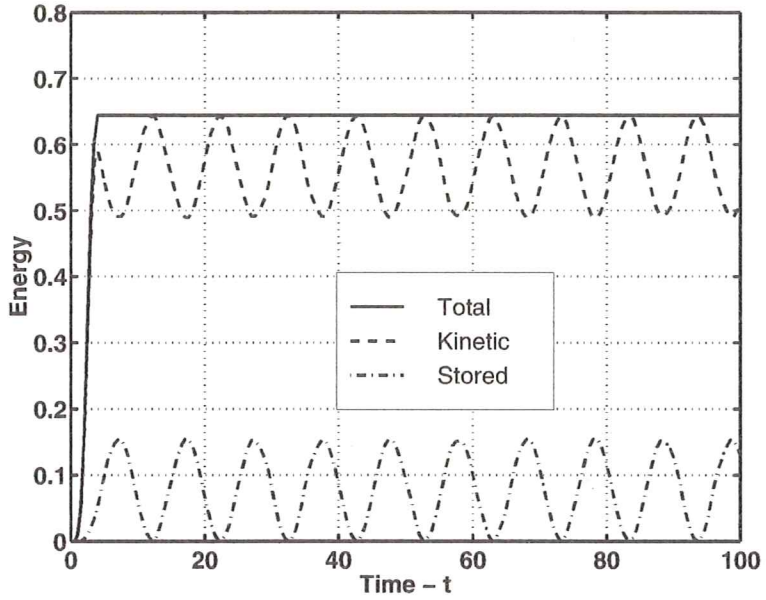

Figure 13: Circular disk with flexible beam attached. Energy behavior.

negative directions. Thus, no resultant force nor couple is applied to the system. The body

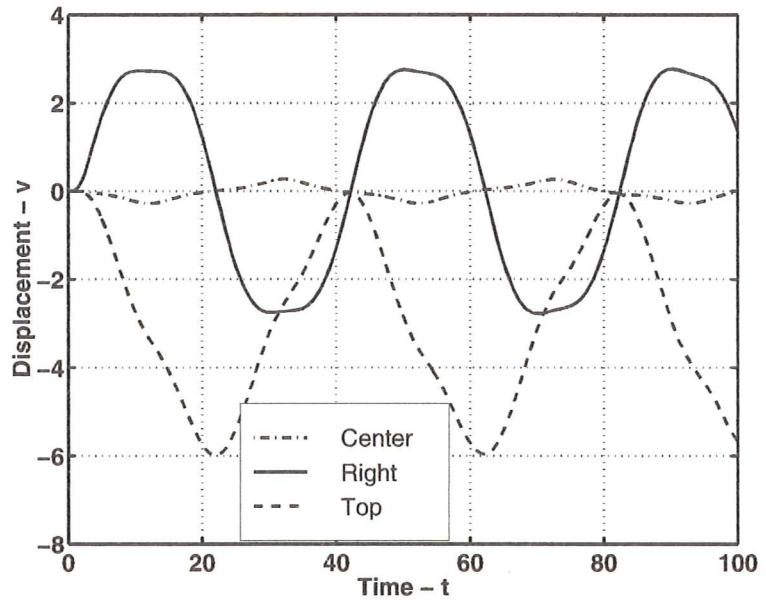

Figure 14: Circular disk with flexible beam attached. Vertical displacement at nodes of simplex.

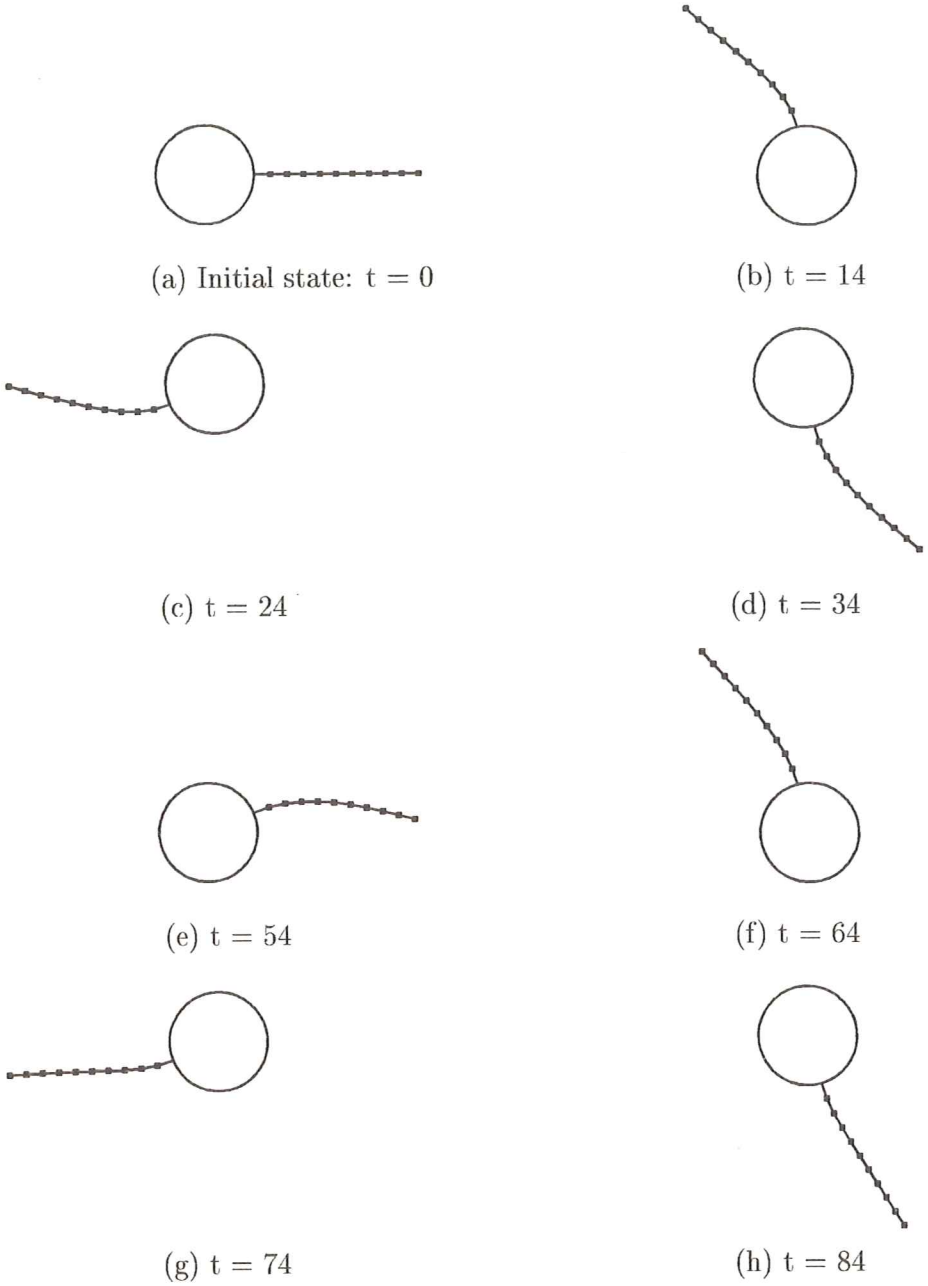

(a) Initial state: t = 0

(b) t = 14

(c) t = 24

(d) t = 34

(e) t = 54

(f) t = 64

(g) t = 74

(h) t = 84

Figure 15: Circular disk with attached beam. Sequence of deformed states.

123 will rotate counterclockwise and the body 245 clockwise with equal angular velocity. A cartoon of the deformed shapes at various times during the first revolution is shown in Fig. 17.

A plot of the vertical displacement for each node is shown in Fig. 18 where it is evident that several revolutions have occurred with pure cyclic motions. It will be noted that the

node 2 also moves in a cyclic, though quite small manner in order to conserve the momentum and energy of the total system. This is apparent from the cartoon in Fig. 17 where we include a fixed node also – the node 2 is seen to oscillate around this point. Finally, a plot of the energy with time is presented in Fig. 19 where is again observed that energy conservation for all times after the loads become zero ($t = 4$) is obtained.

8 Closing remarks

This work has presented an introduction to using translational quantities to represent the motion of rigid and/or flexible bodies. It presents an alternative to using orthogonal matrices to describe the rotational behavior of rigid and structural elements. Here each rigid body is described in terms of a master simplex element using standard finite element isoparametric procedures. Each body is then required to be rigid by constraining the edges of the simplex to maintain their original length. While the method can successfully avoid the introduction of rotational parameters and, thus, the subsequent need to find compatible time discrete integration formulas for such parameters, it introduces the need for additional constraints to impose the rigid body motion. Here we have used Lagrange multiplier methods to include such constraints, however, we also indicated that it was possible to use augmented lagrangian methods for this purpose.

The treatment of rigid multi-body response requires introduction of joints and we have shown how such joints also can be included without need for rotational constraints. Again we use Lagrange multiplier methods to imbed the joint constraints. However, we note that the inclusion of a spherical joint can proceed without the need for introducing constraints if we place a nodes of each simplex master element at the constraint location and give this node the same global number. This is a distinct advantage for the rotation free formulation.

The numerical examples presented in this work are restricted to two-dimensional appli-

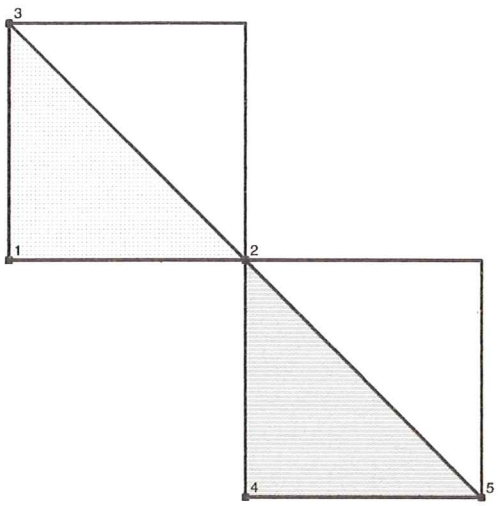

Figure 16: Two square blocks. Connection by revolute joint at node 2.

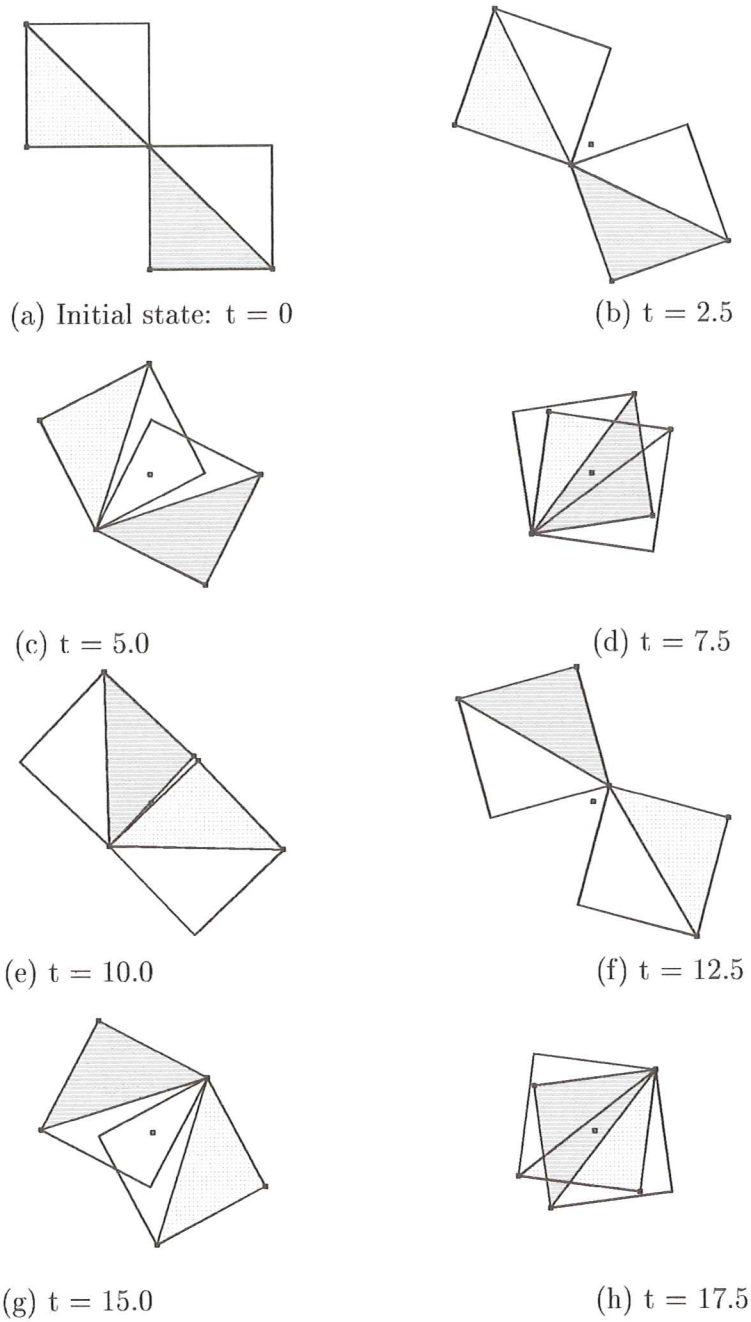

(a) Initial state: t = 0

(b) t = 2.5

(c) t = 5.0

(d) t = 7.5

(e) t = 10.0

(f) t = 12.5

(g) t = 15.0

(h) t = 17.5

Figure 17: Two blocks with revolute joint. Sequence of positions.

cations for simplicity. Extension to three dimensions presents no additional difficulties – contrary to the use of rotation parameters where the difficulties are significant.

Another advantage of the form presented here is that it may be extended to include the class of pseudo-rigid body motions by merely replacing the constraints on constant side length for the simplex to a condition where the stored energy is required to be homogeneous.

Such requirement is trivial using the procedures included here. Indeed the deformation need not be restricted to be homogeneous if higher order behavior is desired. All that is needed is to introduce a form for the master element which includes the polynomial terms desired. This can always be done to any order desired, although at increased cost for each master element formation.

We believe the procedures offered in the present work provide a viable method to develop combined rigid-flexible body analysis systems. One final point is to reiterate the reason for eliminating rotational parameters. Here, we are motivated by the findings of Jelenic and Crisfield who observed differences in the translational and rotational response of a three dimensional beam which was rotated several revolutions. It is our belief that the observed

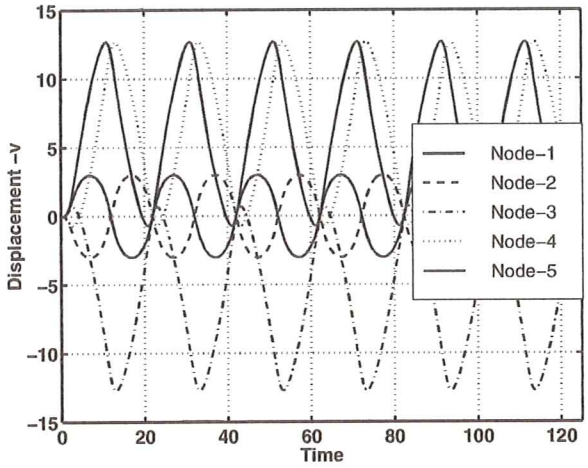

Figure 18: Two square blocks. Vertical displacement of parent simplex nodes.

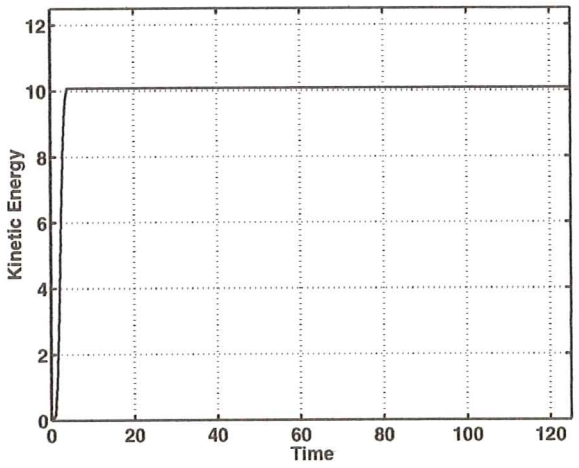

Figure 19: Two square blocks. Kinetic energy vs. time.

response is in fact a discretization error between the rotational parameter integrations and the translational parameters. In duplicating the problem it was observed that the response of all variables was periodic during free motion, however, there was a phase error between those of the rotations and those of the translations which leads to the anomalies noted. Use of the rotational formulation presented here avoids this by always using translational parameters. Should future developments occur which find compatible integration methods for translational and rotational parameters in three-dimensions one can then choose between the more classical previous methods and the one presented here based on other considerations. However, until this occurs the accurate response of structural and rigid-systems requires elimination of the rotational constraints.

References

[1] H. Cohen and R.G. Muncaster. *The Theory of Pseudo-rigid Bodies.* Springer, New York, 1988.

[2] A.A. Shabana. *Dynamics of Multibody Systems.* John Wiley & Sons, New York, 1989.

[3] J.M. Solberg and P. Papadopoulos. A simple finite element-based framework for the analysis of elastic pseudo-rigid bodies. *International Journal for Numerical Methods in Engineering*, 45:1297–1314, 1999.

[4] G.-H. Shi. *Block System Modelling by Discontinuous Deformation Analysis.* Computational Mechanics Publications, Southampton, 1993.

[5] J. Jálon and E. Bayo. *Kinematic and Dynamic Simulation of Multibody Systems.* Springer-Verlag, Heidelberg, 1994.

[6] D.J. Benson and J.O. Hallquist. A simple rigid body algorithm for structural dynamics programs. *International Journal for Numerical Methods in Engineering*, 22:723–749, 1986.

[7] R.A. Wehage and E.J. Haug. Generalized coordinate partitioning for dimension reduction in analysis of constrained dynamic systems. *Journal of Mechanical Design*, 104:247–255, 1982.

[8] A. Cardona and M. Geradin. Beam finite element nonlinear theory with finite rotations. *International Journal for Numerical Methods in Engineering*, 26:2403–2438, 1988.

[9] A. Cardona, M. Geradin, and D.B. Doan. Rigid and flexible joint modelling in multibody dynamics using finite elements. *Computer Methods in Applied Mechanics and Engineering*, 89:395–418, 91.

[10] J.C. Simo and K. Wong. Unconditionally stable algorithms for rigid body dynamics that exactly conserve energy and momentum. *International Journal for Numerical Methods in Engineering*, 31:19–52, 1991. [Addendum: 33:1321-1323, (1992)].

[11] H.T. Clark and D.S. Kang. Application of penalty constraints for multibody dynamics of large space structures. *Advances in the Astronautical Sciences*, 79:511–530, 1992.

[12] G.M. Hulbert. Explicit momentum conserving algorithms for rigid body dynamics. *Computers and Structures*, 44:1291–1303, 1992.

[13] M. Geradin, D.B. Doan, and I. Klapka. MECANO: a finite element software for flexible multibody analysis. *Vehicle system Dynamics*, 22:87–90, 1993. Supplement issue.

[14] S.N. Atluri and A. Cazzani. Rotations in computational solid mechanics. *Archives of Computational Methods in Engineering*, 2:49–138, 1995.

[15] O.A. Bauchau, G. Damilano, and N.J. Theron. Numerical integration of nonlinear elastic multibody systems. *International Journal for Numerical Methods in Engineering*, 38:2727–2751, 1995.

[16] J.A.C. Ambrósio. Dynamics of structures undergoing gross motion and nonlinear deformations: a multibody approach. *Computers and Structures*, 59:1001–1012, 1996.

[17] R.L. Huston. Multibody dynamics since 1990. *Applied Mechanics Reviews*, 49:S35–S40, 1996.

[18] O.A. Bauchau and N.J. Theron. Energy decayiing scheme for non-linear beam models. *Computer Methods in Applied Mechanics and Engineering*, 134:37–56, 1996.

[19] O.A. Bauchau and N.J. Theron. Energy decayiing scheme for non-linear elastic multibody systems. *Computers and Structures*, 59:317–331, 1996.

[20] C. Bottasso and M. Borri. Energy preserving/decaying schemes for nonlinear beam dynamics ausing the helicoidal approximation. *Computer Methods in Applied Mechanics and Engineering*, 143:393–415, 1997.

[21] O.A. Bauchau. Computational schemes for flexible, nonlinear multi-body systems. *Multibody System Dynamics*, 2:169–222, 1998.

[22] O.A. Bauchau and C.L. Bottasso. On the design of energy preserving and decaying schemes for flexible nonlinear multi-body systems. *Computer Methods in Applied Mechanics and Engineering*, 169:61–79, 1999.

[23] O.A. Bauchau and T. Joo. Computational schemes for non-linear elasto-dynamics. *International Journal for Numerical Methods in Engineering*, 45:693–719, 1999.

[24] J.C. García Orden and J.M. Goicolea. Dynamic analysis of rigid and deformable multibody systems with penalty methods and energy-momentum schemes. *Computer Methods in Applied Mechanics and Engineering*, 2000.

[25] I.H. Shames and F.A. Cozzarelli. *Elastic and Inelastic Stress Analysis.* Taylor & Francis, Washington, D.C., 1997. (Revised printing).

[26] A.J. Chen. *Energy-momentum conserving methods for three dimensional dynamic nonlinear multibody systems.* Ph.D thesis, Department of Mechanical Engineering, Stanford University, Stanford, California, 1998. (also SUDMC Report 98-01).

[27] G. Jelenic and M.A. Crisfield. Geometrically exact 3d beam theory: implementation of a strain-invariant finite element for statics and dynamics. *Computer Methods in Applied Mechanics and Engineering*, 171:141–171, 1999.

[28] M. Braun, M. Bischoff, and E. Ramm. Nonlinear shell formulations for complete three-dimensional constitutive laws include composites and laminates. *Computational Mechanics*, 15:1–18, 1994.

[29] E. Ramm. From Reissner plate theory to three dimensions in large deformation shell analysis. *Z. Angew. Math. Mech.*, 79:1–8, 1999.

[30] M. Bischoff and E. Ramm. Solid-like shell or shell-like solid formulation? A personal view. In W. Wunderlich, editor, *Proc. Eur Conf on Comp. Mech (ECCM'99 on CD-ROM)*, Munich, September 1999.

[31] P. Betsch, F. Gruttmann, and E. Stein. A 4-node finite shell element for the implementation of general hyperelastic 3d-elasticity at finite strains. *Computer Methods in Applied Mechanics and Engineering*, 130:57–79, 1996.

[32] O.C. Zienkiewicz and R.L. Taylor. *The Finite Element Method: The Basis*, volume 1. Arnold, London, 5th edition, 2000.

[33] O.C. Zienkiewicz and R.L. Taylor. *The Finite Element Method: Solid Mechanics*, volume 2. Arnold, London, 5th edition, 2000.

[34] R.L. Taylor and A.J.H. Chen. Coupling of rigid and flexible structural components. In *Proc. of the First South African Conference on Mechanics*, Midrand, South Africa, 1996.

[35] O. Gonzalez. *Design and analysis of conserving integrators for nonlinear Hamiltonian systems with symmetry.* Ph.D thesis, Department of Mechanical Engineering, Stanford University, Stanford, California, 1996.

[36] R. A. Nay and S. Utku. An alternative for the finite element method. *Variational Methods in Engineering*, 1, 1972.

[37] E. O nate and M. Cervera. Derivation of thin plate bending elements with one degree of freedom per node: A simple three node triangle. *Engineering Computations*, 10:543–561, 1993b.

[38] E. O nate, F. Zarate, and F. Flores. A simple triangular element for thick and thin plate and shell analysis. *International Journal for Numerical Methods in Engineering*, 37:2569–2582, 1994.

[39] E. O nate and F. Zárate. rotation-free triangular plate and shell elements. *International Journal for Numerical Methods in Engineering*, 47:557–603, 2000.

[40] J.C. Simo and N. Tarnow. The discrete energy-momentum method. conserving algorithm for nonlinear elastodynamics. *Zeitschrift für Mathematik und Physik*, 43:757–793, 1992.

[41] J.C. Simo and N. Tarnow. Exact energy-momentum conserving algorithms and symplectic schemes for nonlinear dynamics. *Computer Methods in Applied Mechanics and Engineering*, 100:63–116, 1992.

[42] J.C. Simo and O. González. Recent results on the numerical integration of infinite dimensional hamiltonian systems. In *Recent Developments in Finite Element Analysis.* CIMNE, Barcelona, Spain, 1994.

[43] J.C. Simo and N. Tarnow. A new energy and momentum conserving algorithm for the non-linear dynamics of shells. *International Journal for Numerical Methods in Engineering*, 37:2527–2549, 1994.

[44] J.C. Simo, N. Tarnow, and M. Doblare. Non-linear dynamics of three-dimensional rods: Exact energy and momentum conserving algorithms. *International Journal for Numerical Methods in Engineering*, 38:1431–1473, 1995.

[45] N. Tarnow. *Energy and momentum conserving algorithms for Hamiltonian systems in the nonlinear dynamics of solids.* PhD thesis, Department of Mechanical Engineering, Stanford University, Stanford, California, 1993.

[46] E.L. Wilson. The static condensation algorithm. *International Journal for Numerical Methods in Engineering*, 8:1974, 199-203.

[47] K.J. Arrow, L. Hurwicz, and H. Uzawa. *Studies in Non-Linear Programming.* Stanford University Press, Stanford, CA, 1958.

[48] H. Goldstein. *Classical Mechanics.* Addison-Wesley, Reading, 2nd edition, 1980.

[49] G.H. Golub and C.F. Van Loan. *Matrix Computations.* The Johns Hopkins University Press, Baltimore MD, 3rd edition, 1996.